

Nanoscale and Macroscale Characterization of the Influence of RAP and RAS on Cracking Resistance of Asphalt Mixes

Munir D. Nazzal, M.ASCE¹; Evan Holcombe²; Sang Soo Kim³; Ala Abbas⁴; and Savas Kaya⁵

Abstract: This paper summarizes the results of laboratory tests that were performed to characterize the blending of recycled asphalt binders [recycled asphalt shingles (RAS) and reclaimed asphalt pavement (RAP) binders] and virgin asphalt binders and to examine the effects of RAP and RAS on the fatigue cracking resistance of asphalt mixtures. Atomic force microscopy (AFM) was used to characterize the interfacial zone that develops between RAP and a virgin asphalt binder and compare it to the interfacial zone that develops between tear-off RAS and the same virgin asphalt binder. Several asphalt mixtures with RAS, RAP, and combinations of the two were also evaluated, including a control mixture (with no RAP or RAS), a mixture containing 30% RAP, a mixture containing 5% tear-off RAS, and a mixture containing 20% RAP and 3% tear-off RAS. A semicircular bend (SCB) test was used to examine the resistance of the asphalt mixtures to fatigue cracking. The AFM test results indicated that blending occurred between the considered RAP and virgin asphalt binders. A reduction in adhesive bonding energy was observed in the blending zone due to the presence of RAP. However, the adhesive bonding energy of the blending zone was significantly higher than the adhesive bonding energy in the RAP binder. The AFM imaging and force spectroscopy experiments revealed no blending between the considered tear-off RAS material and the virgin asphalt binder. The SCB test results showed that the inclusion of the tear-off RAS in the asphalt mixtures considered in this study significantly reduced their fatigue cracking resistance. DOI: 10.1061/(ASCE)MT.1943-5533.0002551. © 2018 American Society of Civil Engineers.

Author keywords: Recycled asphalt shingles (RAS); Reclaimed asphalt pavement (RAP); Cracking; Adhesion; Atomic force microscopy (AFM); Blending.

Background

In recent years, the practice of utilizing reclaimed asphalt pavement (RAP) and recycled asphalt shingles (RAS) individually and together in new asphalt mixtures has increased because of its economic and environmental benefits. In 2014, more than 70 million tons of RAP and about 2 million tons of RAS were used in new asphalt mixtures in the United States. This resulted in more than \$2.6 billion in savings (Hansen and Copeland 2017). The use of RAP and RAS also conserves nonrenewable natural resources (both asphalt and aggregates) and reduces the energy and emissions needed to obtain them. In addition, using RAP and RAS also reduces the amount of construction debris placed into landfills (Copeland 2011).

In recent years, RAS has become a material of interest to the paving community because of its high asphalt binder content. A recent report by the National Asphalt Pavement Association (NAPA)

indicated that the use of RAS increased by about 98% from 2009 to 2016 (Hansen and Copeland 2017). RAS is obtained from two sources: postmanufactured asphalt shingles and postconsumer asphalt shingles. The former are typically referred to as manufacturer scrap, and the latter are generally referred to as tear-offs. About 10 million tons of tear-off RAS is produced annually in the US, but only one million tons of manufacturing waste RAS is generated every year (Nam et al. 2014).

Many research studies have been conducted in recent years to examine the performance of mixtures containing RAS and/or RAP (Ghabchi et al. 2015; Reinke et al. 2014; Zhou et al. 2017; Williams et al. 2013; Cooper et al. 2017). Ghabchi et al. (2015) conducted a study that tested eight surface mixes, four using a PG 64-22 virgin binder and four using a PG 70-28 virgin binder. Each set of four contained a control mix with no RAP or RAS and mixes with 30% RAP, 5% RAP/5% tear-off RAS, and 6% tear-off RAS. It was found that the mixes with 30% RAP and an RAP/RAS blend had better fatigue resistance than the mix with only 6% RAS. Mixtures with tear-off RAS were found to have the highest stiffness as compared to the RAP and control mixes.

Reinke et al. (2014) studied the effects of using RAS on the properties of asphalt mixtures and binders. The results of this study indicated that majority of the unaged RAS mixtures exhibited good performance; however, similar to the virgin control mix, considerable degradation occurred after aging. In addition, the results suggested that the presence of RAS might cause rapid aging of the asphalt binders in mixtures, which could adversely influence the relaxation and low-temperature properties of the binders and the mixtures as well. The authors concluded that mixtures containing RAS had a faster deterioration rate in stiffness and binder properties than those containing RAP only.

¹Associate Professor, Dept. of Civil Engineering, Ohio Univ., Athens, OH 45701 (corresponding author). Email: nazzal@ohio.edu; munir.nazzal@gmail.com

²Graduate Student, Dept. of Civil Engineering, Ohio Univ., Athens, OH 45701.

³Associate Professor, Dept. of Civil Engineering, Ohio Univ., Athens, OH 45701.

⁴Professor, Dept. of Civil Engineering, Univ. of Akron, Akron, OH 44325-3905.

⁵Professor, School of Electrical Engineering and Computer Science, Ohio Univ., Athens, OH 45701.

Note. This manuscript was submitted on April 13, 2018; approved on June 26, 2018; published online on October 11, 2018. Discussion period open until March 11, 2019; separate discussions must be submitted for individual papers. This paper is part of the *Journal of Materials in Civil Engineering*, © ASCE, ISSN 0899-1561.

Zhou et al. (2017) examined the impact of manufacturer waste and tear-off RAS on engineering properties of asphalt mixtures. The study results showed that adding tear-off and manufacturer waste RAS generally resulted in increasing the optimum asphalt content of asphalt mixtures. In addition, the RAS did not have any significant influence on the dynamic modulus of the tested mixes, but improved their resistance to moisture damage and rutting measured by a Hamburg wheel tracking device test. The results of a Texas overlay tester indicated that the mixes with tear-off and manufacturer waste RAS exhibited very poor cracking resistance as compared to those without RAS with either PG 64-22 or PG 70-22, despite the RAS mixes having higher optimum asphalt content (OAC).

Williams et al. (2013) reported the results of a study to characterize the effects of tear-off RAS on the laboratory performance of asphalt mixtures and its compatibility with fractionated recycled asphalt pavement (FRAP). Eight mix designs containing 0% or 5% RAS and varying percentages of FRAP were developed and placed in the pavement shoulder. Beam fatigue and disk compact tension tests were conducted on field-produced laboratory-compacted samples of each of the placed mixes. The beam fatigue test results showed that mixes containing 5% RAS with less than 40% FRAP had satisfactory fatigue cracking performance. The disk compact tension results showed that the low-temperature fracture resistance decreased in the mixes that contained recycled materials.

The current methods used to design asphalt mixtures assume full blending between the aged asphalt binder in RAP and/or RAS materials and the virgin binder in these mixtures. Some studies have shown that blending occurs between the RAP and virgin asphalt binders (Nazzari et al. 2014, 2015, 2018; Nahar et al. 2013). However, the interaction between RAS and virgin asphalt binders is still unclear. This paper compared the blending that occurs between RAP and virgin asphalt binders to the blending that occurs between RAS and virgin binders and determined the effects of blending on the fatigue cracking properties of mixes with RAP and RAS materials. To this end, different atomic force microscopy (AFM) techniques were used to characterize the microstructure, adhesion, and other mechanical properties of the interfacial zone between aged RAP and RAS binders and virgin binders. In addition, semi-circular beam (SCB) tests were performed on the mixtures prepared using the considered RAP, RAS, and virgin asphalt binders in order to examine the effects of RAP and RAS on their resistance to fatigue cracking.

Objectives

The primary objective of this paper was to use AFM to compare the blending that occurs between RAP binder and a virgin asphalt binder to the blending that occurs between RAS and the same virgin asphalt binder. In addition, this paper also uses the results of the AFM to explain the effect of RAP, RAS, and their combination on the macroscale cracking properties of asphalt mixtures.

Testing Program

Recycled Materials

The RAP used in this study was obtained during a resurfacing project on Interstate 270 in Columbus, Ohio. In addition, the tear-off RAS material considered in this study was obtained from a supplier approved by the Ohio Department of Transportation (ODOT). The binder was extracted and recovered from the obtained RAP and RAS materials according to AASHTO R59

Table 1. Performance grade of extracted and recovered RAP/RAS binders

Recovered binder	Continuous low-temperature grade (°C)	Continuous high-temperature grade (°C)
RAP	−23.1	79.7
Tear-off RAS	—	163.9

(AASHTO 2014a) and AASHTO T164 (AASHTO 2014b) tests methods. The performance grade was measured for each of the extracted and recovered binders according to the AASHTO M320 (AASHTO 2017) standard test method. Toluene was the solvent utilized for the extraction of all RAP and RAS binders. Table 1 presents the performance grades for the extracted and recovered RAP and RAS binders. Note that the RAS binder low-temperature performance grade was not determined because it was very difficult to fabricate bending beam rheometer samples from the RAS binder. A virgin asphalt binder with continuous high- and low-temperature grades of 64.9 and 30.6, respectively, and meeting the specifications for PG 64-28 was considered in this study. This is the binder grade used in Ohio in high RAP and RAS mixes.

Tested Mixtures

To examine the effects of the RAS/RAP materials on fatigue cracking performance, a mix that was used in the construction of the intermediate course layer in a resurfacing project on Interstate 270 was selected. The considered asphalt mixture had a 19-mm (0.75-in.) nominal maximum aggregate size (NMAS) and met ODOT specifications for Item 442 Type A (ODOT 2016) for heavy-traffic intermediate mixtures. The selected mixture included PG 64-28 asphalt binder. The aggregate blend of the original mixture used in the field included limestone aggregates, natural sand, and manufactured sand. Several asphalt mixes were designed in order to evaluate the effects of RAP, RAS, and the combination of the two. These included a mixture with no RAP or RAS (control mixture), a mixture with 30% RAP, a mixture with 5% tear-off RAS, and a mixture with 3% tear-off RAS and 20% RAP. The aggregate gradation of the designed mixtures was maintained as close as possible to each other by adjusting the percentage of virgin aggregates in the mixtures. Table 2 presents a summary of the designed mixtures properties.

Microscale Experiments

Atomic force microscopy was used in this study to better understand the blending between RAP/RAS binders and the virgin asphalt binder considered. AFM is a type of scanning probe microscopy technique that involves using a laser-tracked cantilever with a sharp tip to scan over samples. AFM can be used to measure

Table 2. Properties of tested mixes

Mixture	Control	RAP	RAS	RAP and RAS
Virgin binder content	4.7	3.3	4.1	3.2
RAP/RAS binder content	0	1.44	0.9	1.5
Total binder content	4.7	4.7	5.0	4.7
RAP/RAS replacement ratio ^a	0.00	0.30	0.18	0.32
VMA	13.1	13.0	13.8	13.2
% RAP	0	30	0	20
% RAS	0	0	5	3

Note: VMA = void in mineral aggregate.

^aThis is defined as the ratio of RAP/RAS binder in the mix divided by the total binder content of the mix.

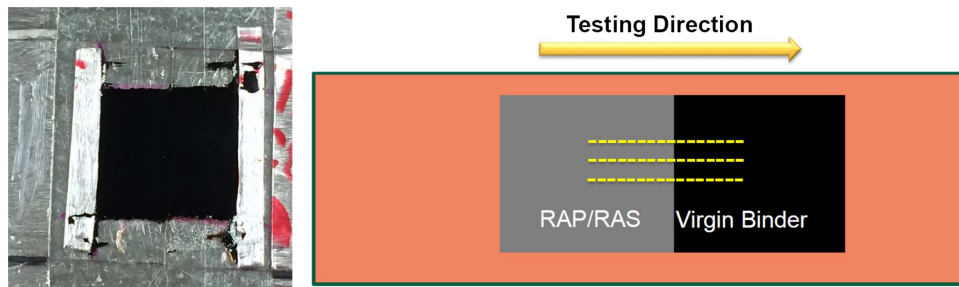


Fig. 1. AFM samples prepared and tested in this study.

microscale forces within different types of materials (Fischer-Cripps 2006). It has become increasingly useful in testing engineering materials such as viscoelastic asphalt binders in order to understand nanomechanical properties (Nazzal et al. 2012; Pauli et al. 2014; Nazzal et al. 2014; Holcombe et al. 2017). AFM can be used to accurately map a particular force in various imaging modes with nanometer resolution or to track the dependence of different components as a function of tip-surface distance with sub-nanometer resolution. The following subsections provide details of the experiments performed in this study.

Preparation of AFM Specimens

AFM specimens were prepared using a procedure developed in a previous study to simulate the interaction that occurs between RAP/RAS and virgin binders in an asphalt mix during its production (Nazzal et al. 2018). In this procedure, a predetermined amount of a binder was placed on a glass microscope slide that was broken in half and tightly attached together at the opposite ends using aluminum tape. The weight of each binder was determined by multiplying the specific gravity of the binder by the volume of the constraint on the slide. Once the proper weight was placed on the confined glass slide, the samples were heated on a hot plate for a specific time and at a specific temperature. The RAP and virgin binders were soft enough after heating at 153°C for 5 min to spread and ensure the development of a smooth surface for testing. However, the tear-off RAS binders were much stiffer and required a longer heating time of 2 h at a higher temperature of 210°C, along with added weight on top of the samples, in order to spread the binder over the surface. A small piece of Teflon paper was placed between the weight and the RAS binder to prevent the binder from sticking to the weight. After the slides with different binders were prepared, they were allowed to cool down to room temperature. The tape longitudinal to the slide was removed and the two halves of the slide were separated. The edges of the slides were finely cleaned to ensure optimal blending without contamination. The slides with recycled materials (RAP or RAS) were then heated on a hot plate for 30 s at 153°C. This was done in order to simulate the heating of RAP before the addition of virgin binder. Next, the slide with the virgin asphalt binder was quickly pressed against the edge of the recycled binder slide. The assembly of two slides was heated on top of a hot plate for 3 min at 153°C immediately after they were combined together. This caused the melting and spreading of the asphalt binders on both slides, which created a thin film with an interfacial zone at the middle.

AFM Experiments

An Agilent 5500LS AFM (Palo Alto, California) was used to perform all the AFM experiments in this study. Two AFM techniques were used in this study: AFM force spectroscopy and AFM imaging. Force spectroscopy experiments were performed at a temperature of $24 \pm 1^\circ\text{C}$ in order to measure the elastic modulus and

bonding energy for the different RAP/RAS and virgin binder combinations. In these experiments, the tip penetrated the sample surface to a specific indentation depth and was then retracted away from the sample surface. The selected indentation depth was around $0.3 \mu\text{m}$, which was less than 10% of the sample thickness, in order to minimize any boundary effects from the glass slide. The force spectroscopy tests were conducted at a constant test duration of 2 s for all indentation experiments. Micromasch HQ:NSC19/AL BS (Watsonville, California) tips were used for all tested samples. The cantilever for these tips had an average frequency of 90 kHz, a spring constant ranging from 1.5 to 2 N/m, a length of $125 \pm 5 \mu\text{m}$, a width of $22.5 \pm 3 \mu\text{m}$, and a thickness of $1 \pm 0.5 \mu\text{m}$.

Force spectroscopy experiments were performed for each sample combination by testing different points along a straight line over the sample surface. As shown in Fig. 1, testing started at the RAP or RAS binder zone toward the interface and into the virgin asphalt binder zone. The tested point spacing was higher in the RAP binder zone but was significantly reduced as the blending zone was approached in order to capture any change in the binder properties. Within the blending zone, the spacing between tested points ranged between 5 and $30 \mu\text{m}$. At least two replicate samples were tested for each RAP/RAS and virgin binder combination, and two lines of data were collected for each of the two samples.

The outcome of a single indentation in a force spectroscopy experiment is a force-distance curve similar to the one presented in Fig. 2. The curve is divided into two parts: the approaching part and the retracting part. First, the tip approaches the sample surface; as the tip gets closer to the surface, the force between the tip and

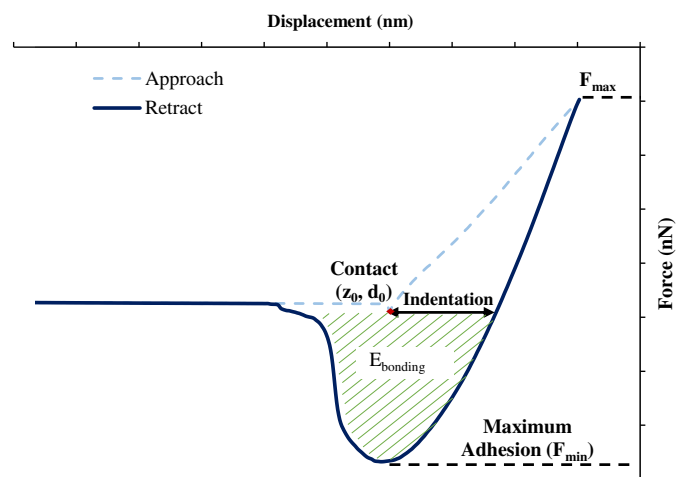


Fig. 2. Typical force-distance curve obtained in a force spectroscopy experiment.

the sample starts to increase slightly. As soon as the tip contacts the surface, a significant increase in the deflection of the cantilever occurs. The tip then continues to penetrate the sample to the preselected indentation depth. The maximum observed positive force is reached at the maximum indentation point. The tip is then retracted from the sample surface until it overcomes the adhesive forces between the tip and asphalt and completely snaps off the asphalt sample.

The results of the force spectroscopy tests were analyzed to obtain the reduced elastic modulus of the asphalt binder E_{reduced} and the bonding energy E_{bonding} . Eq. (1) was used to compute E_{reduced} (Fischer-Cripps 2006). In addition, E_{bonding} , which is the total energy needed to separate the tip from the asphalt sample, was calculated using Eq. (3). This equation represents the area under the force-distance curve in the retraction region where the force was less than zero (Pauli et al. 2014), as indicated by the shaded portion of Fig. 2

$$E_{\text{reduced}} = \frac{\pi}{2} \frac{F}{\delta^2 \tan(\alpha)} \quad (1)$$

$$\delta = z - d \quad (2)$$

where F = measured force; δ = indentation depth; α = half-opening angle of the AFM tip; d = deflection of the cantilever; and z = displacement of the piezo driver

$$E_{\text{bonding}} = \int_{z_0}^{z_1} F dz \approx \frac{\Delta z}{2N} \sum_{i=1}^N [F(z_{i+1}) + F(z_i)] \quad (3)$$

AFM images were taken during the testing of the prepared samples. A minimum of two images were obtained within the RAP/RAS binder zone, the blending zone, and the virgin asphalt binder zone. The AFM images were taken in the tapping mode rather than the contact mode in order to prevent any damage to the relatively soft asphalt binders.

Macroscale Tests: Semicircular Bending Test

Semicircular bending tests were performed on each mixture in order to evaluate fatigue cracking performance at an intermediate temperature of 25°C. The SCB tests were performed according to ASTM D8044 (ASTM 2016). An Instron Auto SCB (Instron Research, Triangle Park, North Carolina) was used to conduct all SCB tests. The SCB tests were conducted on samples that were long-term aged according to AASHTO R30 (AASHTO 2002)

by placing them in an environmental chamber for 5 days at 85°C. Samples had to be tested at three different notch depths (25.4, 31.8, and 38.1 mm) in this SCB method. At least four samples had to be tested for each notch depth. The SCB tests were conducted by loading the samples to failure using a 0.5 mm/min deformation rate. The fracture energy needed to cause failure was determined for each sample by computing the area under the load versus displacement curve up to the peak load. The critical strain energy release rate J_c was calculated using Eq. (4) the average strain energy per thickness of the sample with each notch depth

$$J_c = \frac{-1}{b} \left(\frac{dU}{da} \right) \quad (4)$$

where b = sample thickness (m); a = sample notch depth (m); and U = strain energy up to peak load of failure (kJ).

Results and Analysis

Results of AFM Imaging

RAP Samples

AFM images were obtained during the testing of the different types of extracted and recovered samples. Figs. 3(a–c) present representative phase images of the RAP, interfacial blending zone, and virgin asphalt binder (PG 64-28) that were obtained for extracted RAP samples. It is clear that the microstructure of the RAP binder was different from that of the virgin asphalt binder, such that the size of the beelike structure in the considered RAP binders was significantly smaller than in the virgin asphalt binder. This may be attributed to the aging of the RAP binder, which may have resulted in obstructing the movement of asphalt molecule chains and in preventing the crystallization of microcrystalline waxes and waxy molecules. Fig. 3(b) shows the interfacial zone that develops between the RAP and virgin asphalt binders. It is clear that the microstructure of the interfacial zone was different from the microstructure of both the RAP and virgin asphalt binder and was affected by those binders. The beelike structure of the interfacial zone was larger than that of the RAP asphalt binder but much smaller than that of the virgin binder. In addition, the phase contrast between dispersed domains and flat matrix observed for the virgin binder seemed to be inverted. Hence, Figs. 3(a–c) clearly suggest that there was some blending at the interface between the RAP and virgin binders, which occurred on the microscale level in a fairly uniform manner.

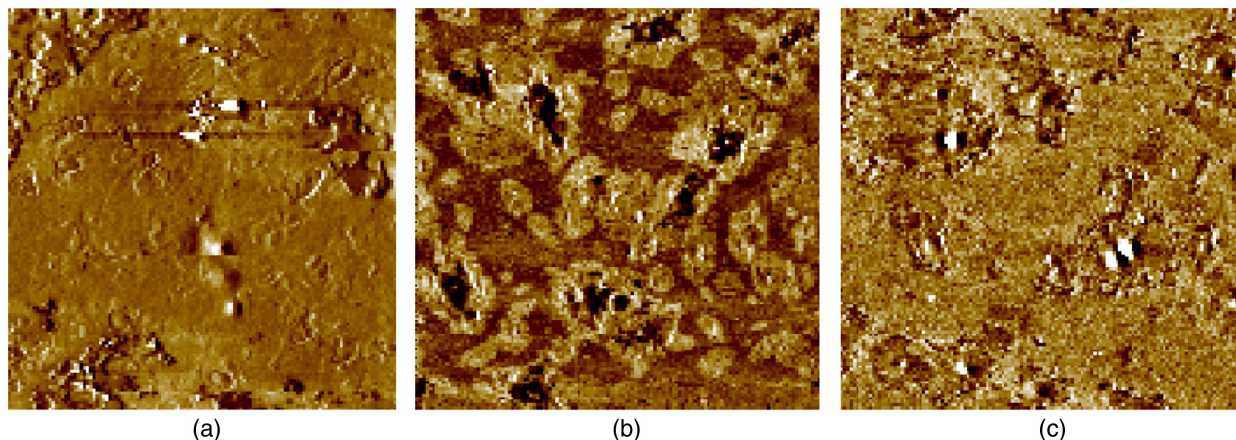


Fig. 3. AFM phase imaging of (a) RAP binder zone; (b) blending zone; and (c) virgin binder.

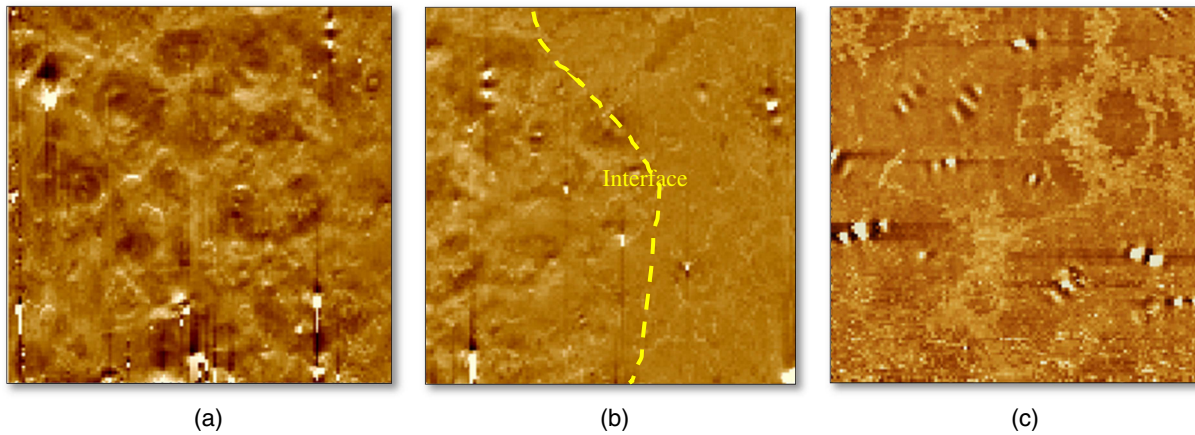


Fig. 4. AFM phase imaging of (a) tear-off RAS zone; (b) blending zone; and (c) PG 64-28 virgin asphalt binder.

RAS Samples

AFM images were also obtained for the RAS samples. Figs. 4(a–c) show the phase images for RAS specimens. The RAS binder [Fig. 4(a)] had a different nanostructure than the virgin PG 64-28 asphalt binder [Fig. 4(c)]. Fig. 4(b) shows the interface between the RAS and the virgin asphalt binder. A clear distinction between the RAS and the virgin asphalt binder can be seen within the interfacial zone. This indicates that no blending occurred between the two asphalt binders. The interfacial zone shown in Fig. 4(b) suggests that the zone contained RAS and virgin binder domains that did not blend.

Results of Force Spectroscopy Experiments

RAP Samples

The reduced modulus and bonding energy values were plotted with distance along the sample. Figs. 5 and 6 present typical curves for reduced modulus and bonding energy obtained from the AFM force spectroscopy tests. As seen in Fig. 5, the curve for any combination starts with the reduced modulus of RAP binder where the slope of the curve is constant and the modulus is high. Once the blending zone is approached, a gradual decrease in the modulus values occurs and the slope of the curve begins to drop until it reaches an asymptote representing the virgin binder reduced modulus. Fig. 5 also shows the average values of the reduced moduli for the RAP binder, the blending interfacial zone, and the virgin asphalt binder.

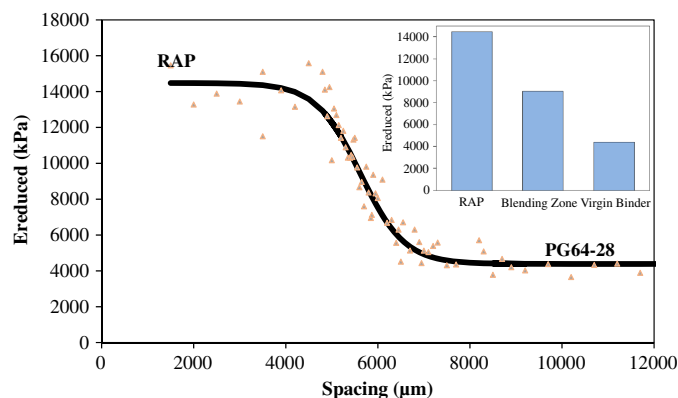


Fig. 5. Reduced modulus results for RAP blended binders.

The modulus of the blending zone was between those of the RAP and virgin binder moduli but slightly closer to the virgin binder (PG 64-28).

Fig. 6 shows the variation of the bonding energy with distance across the samples for RAP and virgin binder. The curve showed behavior opposite to that of the reduced modulus curve. The curve starts with the low bonding energy values for the RAP binder. The bonding energy begins to increase when the blending zone is reached, as shown by the sharp increase in the slope curve, and it reaches constant values over the virgin binder, which had much higher bonding energy than the RAP binder. The blending zones based on the reduced stiffness modulus values were also very similar in size, much like the bonding-energy-based blending zone. This result helped verify the consistency of the blending zone size determination based on two different nanomechanical properties. Fig. 6 also shows the average adhesive bonding energy values for the RAP binder, the blending interfacial zone, and the virgin asphalt binder. The adhesive bonding energy of the blending zone was lower than that of the virgin binder. However, the blending zone had a higher bonding energy than the RAP binder.

RAS Samples

Figs. 7 and 8 present typical curves of the reduced modulus and bonding energy values, respectively, obtained from force spectroscopy tests for tear-off RAS samples. The reduced modulus curve shown in Fig. 7 starts with high values for the RAS binder. This is followed by a sudden drop when the interface with the virgin binder

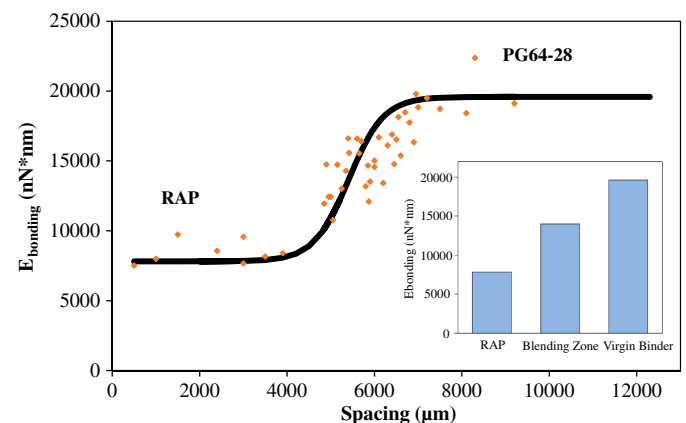


Fig. 6. Bonding energy results for RAP blended binders.

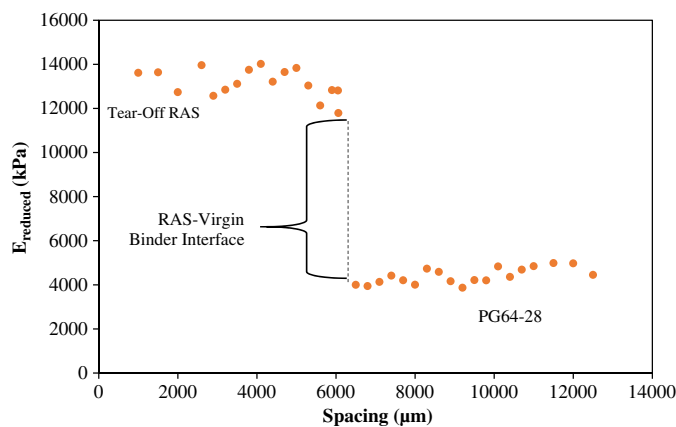


Fig. 7. Reduced modulus curve for tear-off RAS samples.

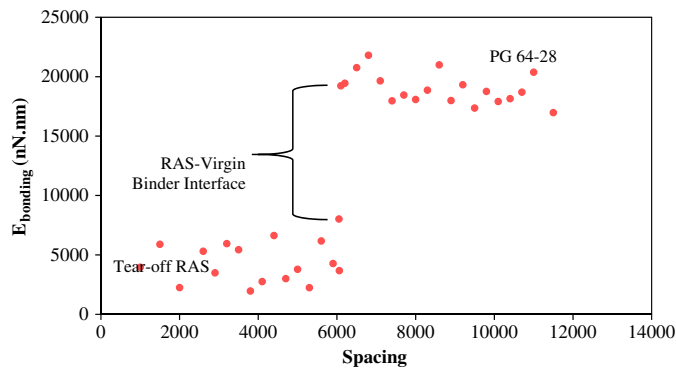


Fig. 8. Bonding energy curve for tear-off RAS samples.

is reached. The bonding energy curves show a trend similar to what is seen with the reduced modulus curves; however, the bonding energy curves start with low bonding energy values for the RAS binder that drastically increase when the interface with the virgin binder is reached. The reduced modulus and bonding energy curves clearly indicate that no blending occurred between the tear-off RAS and the virgin binder considered in this study. This confirms the results obtained from the AFM images presented in Fig. 4. The lack of blending between the virgin binders and the RAS binders at mixing temperatures are thought to contribute to poor fatigue cracking resistance at intermediate temperatures.

SCB Test Results

The SCB test was performed on long-term aged samples to evaluate the fracture resistance of mixtures with recycled materials at aged conditions. The slope of the linear fit for each notch depth was found to be very sensitive to the peak loading of each sample. Fig. 9 presents the average calculated J integral value (J_{Ic}) values for the considered mixes. The control mixture with virgin materials only had the higher critical fracture resistance values compared to mixes with RAP and/or RAS. In addition, the mixture with RAS only had significantly lower fracture resistance values compared to other mixtures with RAP. These results confirmed the AFM experiment findings that showed that the tear-off RAS did not blend with the virgin asphalt binder considered. This suggests that the assumption during mix design that tear-off RAS binders blend with virgin asphalt binders is inaccurate and may result in mixes that are more prone to fatigue cracking. Mohammad et al. (2012) recommended a minimum value of 0.5 kJ/m² for well performing asphalt mixes.

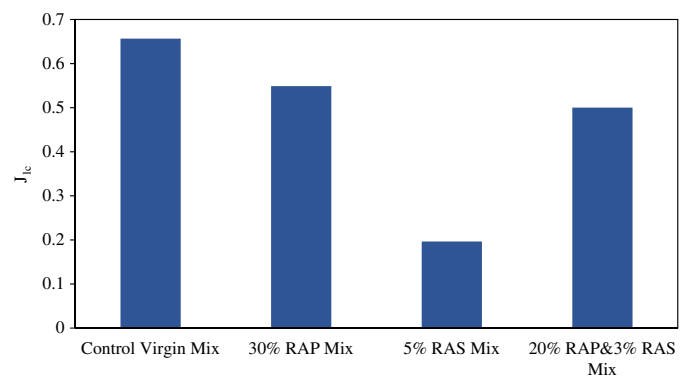


Fig. 9. Calculated J -integral values for asphalt mixes.

Note that the control mixture and the mixture with 30% RAP had an acceptable fracture resistance based on that criterion; however, the mixture with 5% tear-off RAS did not meet this criterion and had a J_{Ic} value that was much lower than the recommended minimum value.

Conclusions

This paper summarized the results of a study that involved using AFM to characterize the blending between recycled materials (RAP/RAS) and virgin asphalt binders. In addition, the cracking resistance of mixtures prepared using the RAP, RAS, and virgin binders considered was evaluated. Based on the results presented in this paper, the following conclusions can be drawn:

- The results of the AFM imaging and force spectroscopy experiments conducted on the RAP and the virgin binder indicated that the RAP binders blended with the considered virgin asphalt binder in a blending zone.
- The bonding energy of the blending zone was higher than that of the RAP binder but lower than that of the virgin asphalt binder, which indicated that the RAP binder adversely affected the adhesive properties of the virgin asphalt that it blended with.
- The AFM images of RAS samples indicated that no blending occurred between the tear-off RAS and the virgin asphalt binders considered in this study. This result was also confirmed in the AFM force spectroscopy experiments.
- The SCB test results showed that the mixture with 30% RAP had acceptable fatigue cracking resistance.
- The results of the SCB tests conducted on the asphalt mixtures considered in this study indicated that the use of 5% tear-off RAS adversely affected the fatigue cracking resistance of the mixes. It is recommended that additional asphalt mixtures with different binder types should be tested in the future in order to validate the results obtained in this paper.
- The SCB tests were able to detect the influence of RAS on the fatigue cracking properties of the asphalt mixtures.
- The assumption that the binder in tear-off RAS blends with virgin asphalt binder as does RAP binder may be inaccurate.

References

- AASHTO. 2002. *Standard practice for mixture conditioning of hot mix asphalt*. AASHTO R30. Washington, DC: AASHTO.
- AASHTO. 2014a. *Standard method of recovery of asphalt binder from solution by Abson method*. AASHTO R59. Washington, DC: AASHTO.

- AASHTO. 2014b. *Standard method of test for quantitative extraction of asphalt binder from hot mix asphalt*. AASHTO T164. Washington, DC: AASHTO.
- AASHTO. 2017. *Standard specification for performance-graded asphalt binder*. AASHTO M320. Washington, DC: AASHTO.
- ASTM. 2016. *Standard test method for evaluation of asphalt mixture cracking resistance using the semi-circular bend test (SCB) at intermediate temperatures*. ASTM D8044. West Conshohocken, PA: ASTM.
- Cooper, S., Jr., L. Mohammad, and M. Elseifi. 2017. "Laboratory performance of asphalt mixtures containing recycled asphalt shingles, reclaimed asphalt pavement, and recycling agents." *J. Mater. Civ. Eng.* 29 (3): D4016001. [https://doi.org/10.1061/\(ASCE\)MT.1943-5533.0001658](https://doi.org/10.1061/(ASCE)MT.1943-5533.0001658).
- Copeland, A. 2011. *Reclaimed asphalt pavement in asphalt mixtures: State of the practice*. Rep. No. FHWA-HRT-11-021. Washington, DC: FHWA.
- Fischer-Cripps, A. C. 2006. "Critical review of analysis and interpretation of nanoindentation test data." *Surf. Coat. Technol.* 200 (14): 4153–4165. <https://doi.org/10.1016/j.surfcoat.2005.03.018>.
- Ghabchi, R., D. Singh, M. Zaman, and Z. Hossain. 2015. "Laboratory characterization of asphalt mixes containing RAP and RAS." *Int. J. Pavement Eng.* 17 (9): 829–846. <https://doi.org/10.1080/10298436.2015.1022778>.
- Hansen, K. R., and A. Copeland. 2017. *Asphalt pavement industry survey on recycled materials and warm-mix asphalt usage 2016: Information series 138*. 7th ed. Lanham, MD: National Asphalt Pavement Association.
- Holcombe, E. W., M. D. Nazzal, W. Mogawer, A. J. Austerman, and S. Kaya. 2017. "Evaluating asphalt binders prepared with different processes to meet the same performance grade: Use of atomic force microscope." *Transp. Res. Rec.* 2632: 99–109. <https://doi.org/10.3141/2632-11>.
- Mohammad, L. N., M. Kim, and M. Elseifi. 2012. "Characterization of asphalt mixture's fracture resistance using the semi-circular bending (SCB) test." In *Proc., 7th RILEM Int. Conf. on Cracking in Pavements*, 1–10. Dordrecht, Netherlands: Springer.
- Nahar, S., M. Mohajeri, A. Schmets, A. Scarpas, M. Van De Ven, and G. Schitter. 2013. "First observation of blending-zone morphology at interface of reclaimed asphalt binder and virgin bitumen." *Transp. Res. Rec.* 2370: 1–9. <https://doi.org/10.3141/2370-01>.
- Nam, B., H. Maherinia, and A. Behzadan. 2014. "Mechanical characterization of asphalt tear-off roofing shingles in hot mix asphalt." *J. Constr. Build. Mater.* 50: 308–316. <https://doi.org/10.1016/j.conbuildmat.2013.08.037>.
- Nazzal, M. D., E. Holcombe, S. S. Kim, A. Abbas, and S. Kaya. 2018. "Multi-scale evaluation of the effect of RAS on the fracture properties of asphalt mixtures." *Constr. Build. Mater.* 175: 126–133. <https://doi.org/10.1016/j.conbuildmat.2018.04.080>.
- Nazzal, M. D., S. Kaya, T. Gunay, and P. Ahmedzade. 2012. "Fundamental characterization of asphalt clay nanocomposites." *J. Nanomech. Micromech.* 3 (1): 1–8. [https://doi.org/10.1061/\(ASCE\)NM.2153-5477.0000050](https://doi.org/10.1061/(ASCE)NM.2153-5477.0000050).
- Nazzal, M. D., W. Mogawer, A. Austerman, L. A. Qtaish, and S. Kaya. 2015. "Multi-scale evaluation of the effect of rejuvenators on the performance of high RAP content mixtures." *Constr. Build. Mater.* 101: 50–56. <https://doi.org/10.1016/j.conbuildmat.2015.10.029>.
- Nazzal, M. D., W. Mogawer, S. Kaya, and T. Bennert. 2014. "Multiscale evaluation of the composite asphalt binder in high-reclaimed asphalt pavement mixtures." *J. Mater. Civ. Eng.* 26 (7): 04014019. [https://doi.org/10.1061/\(ASCE\)MT.1943-5533.0000825](https://doi.org/10.1061/(ASCE)MT.1943-5533.0000825).
- ODOT (Ohio Department of Transportation). 2016. *Constriction and materials specifications*. Item 442 Type A. Columbus, OH: ODOT.
- Pauli, T., W. Grimes, A. Cookman, and S. Huang. 2014. "Adherence energy of asphalt thin films measured by force-displacement atomic force microscopy." *J. Mater. Civ. Eng.* 26 (12): 04014089. [https://doi.org/10.1061/\(ASCE\)MT.1943-5533.0001003](https://doi.org/10.1061/(ASCE)MT.1943-5533.0001003).
- Reinke, G., S. Glidden, S. Engber, S. Ryan, and D. Herlitzka. 2014. "Impact on the use of reclaimed asphalt shingles on mixture and recovered binder properties." In *Proc., 2014 ISAP Conf.* Lino Lakes, MN: International Society for Asphalt Pavements.
- Williams, R. C., A. A. Cascione, J. Yu, D. Haugen, M. Marasteanu, and J. McGraw. 2013. *Performance of recycled asphalt shingles in hot mix asphalt*. Final Rep. for Pooled Fund Study TPF 5(213). Ames, IA: Institute of Transportation, Iowa State Univ.
- Zhou, F., S. Im, S. Hu, D. Newcomb, and T. Scullion. 2017. "Selection and preliminary evaluation of laboratory cracking tests for routine asphalt mix designs." *Road Mater. Pavement Des.* 1–15. <https://doi.org/10.1080/14680629.2017.1396236>.